Observation of J/ψ→pp[over ¯]a_{0}(980) at BESIII

M. Ablikim *et al.* (BESIII Collaboration)

Observation of $J/\psi \to p\bar{p}a_0(980)$ at BESIII

M. Ablikim[1], M. N. Achasov[8,a], X. C. Ai[1], O. Albayrak[4], M. Albrecht[3], D. J. Ambrose[42], F. F. An[1], Q. An[43], J. Z. Bai[1], R. Baldini Ferroli[19A], Y. Ban[29], D. W. Bennett[18], J. V. Bennett[18], M. Bertani[19A], D. Bettoni[20A], J. M. Bian[41], F. Bianchi[46A,46C], E. Boger[22,f], O. Bondarenko[23], I. Boyko[22], S. Braun[38], R. A. Briere[4], H. Cai[48], X. Cai[1], O. Cakir[37A], A. Calcaterra[19A], G. F. Cao[1], S. A. Cetin[37B], J. F. Chang[1], G. Chelkov[22,b], G. Chen[1], H. S. Chen[1], J. C. Chen[1], M. L. Chen[1], S. J. Chen[27], X. Chen[1], X. R. Chen[24], Y. B. Chen[1], H. P. Cheng[16], X. K. Chu[29], Y. P. Chu[1], G. Cibinetto[20A], D. Cronin-Hennessy[41], H. L. Dai[1], J. P. Dai[1], D. Dedovich[22], Z. Y. Deng[1], A. Denig[21], I. Denysenko[22], M. Destefanis[46A,46C], F. De Mori[46A,46C], Y. Ding[25], C. Dong[28], J. Dong[1], L. Y. Dong[1], M. Y. Dong[1], S. X. Du[50], J. Z. Fan[36], J. Fang[1], S. S. Fang[1], Y. Fang[1], L. Fava[46B,46C], G. Felici[19A], C. Q. Feng[43], E. Fioravanti[20A], C. D. Fu[1], O. Fuks[22,f], Q. Gao[1], Y. Gao[36], I. Garzia[20A], C. Geng[43], K. Goetzen[9], W. X. Gong[1], W. Gradl[21], M. Greco[46A,46C], M. H. Gu[1], Y. T. Gu[11], Y. H. Guan[1], L. B. Guo[26], T. Guo[26], Y. P. Guo[21], Z. Haddadi[23], S. Han[48], Y. L. Han[1], F. A. Harris[40], K. L. He[1], M. He[1], Z. Y. He[28], T. Held[3], Y. K. Heng[1], Z. L. Hou[1], C. Hu[26], H. M. Hu[1], J. F. Hu[46A], T. Hu[1], G. M. Huang[5], G. S. Huang[43], H. P. Huang[48], J. S. Huang[14], L. Huang[1], X. T. Huang[31], Y. Huang[27], T. Hussain[45], C. S. Ji[43], Q. Ji[1], Q. P. Ji[28], X. B. Ji[1], X. L. Ji[1], L. L. Jiang[1], L. W. Jiang[48], X. S. Jiang[1], J. B. Jiao[31], Z. Jiao[16], D. P. Jin[1], S. Jin[1], T. Johansson[47], A. Julin[41], N. Kalantar-Nayestanaki[23], X. L. Kang[1], X. S. Kang[28], M. Kavatsyuk[23], B. C. Ke[4], B. Kloss[21], B. Kopf[3], M. Kornicer[40], W. Kuehn[38], A. Kupsc[47], W. Lai[1], J. S. Lange[38], M. Lara[18], P. Larin[13], M. Leyhe[3], C. H. Li[1], Cheng Li[43], Cui Li[43], D. Li[17], D. M. Li[50], F. Li[1], G. Li[1], H. B. Li[1], J. C. Li[1], Jin Li[30], K. Li[31], K. Li[12], P. R. Li[39], Q. J. Li[1], T. Li[31], W. D. Li[1], W. G. Li[1], X. L. Li[31], X. N. Li[1], X. Q. Li[28], Z. B. Li[35], H. Liang[43], Y. F. Liang[33], Y. T. Liang[38], D. X. Lin[13], B. J. Liu[1], C. L. Liu[4], C. X. Liu[1], F. H. Liu[32], Fang Liu[1], Feng Liu[5], H. B. Liu[11], H. H. Liu[15], H. M. Liu[1], J. Liu[1], J. P. Liu[48], K. Liu[36], K. Y. Liu[25], P. L. Liu[31], Q. Liu[39], S. B. Liu[43], X. Liu[24], Y. B. Liu[28], Z. A. Liu[1], Zhiqiang Liu[1], Zhiqing Liu[21], H. Loehner[23], X. C. Lou[1,c], H. J. Lu[16], H. L. Lu[1], J. G. Lu[1], Y. Lu[1], Y. P. Lu[1], C. L. Luo[26], M. X. Luo[49], T. Luo[40], X. L. Luo[1], M. Lv[1], X. R. Lyu[39], F. C. Ma[25], H. L. Ma[1], Q. M. Ma[1], S. Ma[1], T. Ma[1], X. Y. Ma[1], F. E. Maas[13], M. Maggiora[46A,46C], Q. A. Malik[45], Y. J. Mao[29], Z. P. Mao[1], S. Marcello[46A,46C], J. G. Messchendorp[23], J. Min[1], T. J. Min[1], R. E. Mitchell[18], X. H. Mo[1], Y. J. Mo[5], H. Moeini[23], C. Morales Morales[13], K. Moriya[18], N. Yu. Muchnoi[8,a], H. Muramatsu[41], Y. Nefedov[22], F. Nerling[13], I. B. Nikolaev[8,a], Z. Ning[1], S. Nisar[7], X. Y. Niu[1], S. L. Olsen[30], Q. Ouyang[1], S. Pacetti[19B], P. Patteri[19A], M. Pelizaeus[3], H. P. Peng[43], K. Peters[9], J. L. Ping[26], R. G. Ping[1], R. Poling[41], M. Qi[27], S. Qian[1], C. F. Qiao[39], L. Q. Qin[31], N. Qin[48], X. S. Qin[1], Y. Qin[29], Z. H. Qin[1], J. F. Qiu[1], K. H. Rashid[45], C. F. Redmer[21], M. Ripka[21], G. Rong[1], X. D. Ruan[11], V. Santoro[20A], A. Sarantsev[22,d], M. Savrié[20B], K. Schoenning[47], S. Schumann[21], W. Shan[29], M. Shao[43], C. P. Shen[2], X. Y. Shen[1], H. Y. Sheng[1], M. R. Shepherd[18], W. M. Song[1], X. Y. Song[1], S. Spataro[46A,46C], B. Spruck[38], G. X. Sun[1], J. F. Sun[14], S. S. Sun[1], Y. J. Sun[43], Y. Z. Sun[1], Z. J. Sun[1], Z. T. Sun[43], C. J. Tang[33], X. Tang[1], I. Tapan[37C], E. H. Thorndike[42], M. Tiemens[23], D. Toth[41], M. Ullrich[38], I. Uman[37B], G. S. Varner[40], B. Wang[28], D. Wang[29], D. Y. Wang[29], K. Wang[1], L. L. Wang[1], L. S. Wang[1], M. Wang[31], P. Wang[1], P. L. Wang[1], Q. J. Wang[1], S. G. Wang[29], W. Wang[1], X. F. Wang[36], Y. D. Wang[19A], Y. F. Wang[1], Y. Q. Wang[21], Z. Wang[1], Z. G. Wang[1], Z. H. Wang[43], Z. Y. Wang[1], D. H. Wei[10], J. B. Wei[29], P. Weidenkaff[21], S. P. Wen[1], M. Werner[38], U. Wiedner[3], M. Wolke[47], L. H. Wu[1], N. Wu[1], Z. Wu[1], L. G. Xia[36], Y. Xia[17], D. Xiao[1], Z. J. Xiao[26], Y. G. Xie[1], Q. L. Xiu[1], G. F. Xu[1], L. Xu[1], Q. J. Xu[12], Q. N. Xu[39], X. P. Xu[34], Z. Xue[1], L. Yan[43], W. B. Yan[43], W. C. Yan[43], Y. H. Yan[17], H. X. Yang[1], L. Yang[48], Y. Yang[5], Y. X. Yang[10], H. Ye[1], M. Ye[1], M. H. Ye[6], B. X. Yu[1], C. X. Yu[28], H. W. Yu[29], J. S. Yu[24], S. P. Yu[31], C. Z. Yuan[1], W. L. Yuan[27], Y. Yuan[1], A. Yuncu[37B,e], A. A. Zafar[45], A. Zallo[19A], S. L. Zang[27], Y. Zeng[17], B. X. Zhang[1], B. Y. Zhang[1], C. Zhang[27], C. B. Zhang[17], C. C. Zhang[1], D. H. Zhang[1], H. H. Zhang[35], H. Y. Zhang[1], J. J. Zhang[1], J. Q. Zhang[1], J. W. Zhang[1], J. Y. Zhang[1], J. Z. Zhang[1], S. H. Zhang[1], X. J. Zhang[1], X. Y. Zhang[31], Y. Zhang[1], Y. H. Zhang[1], Z. H. Zhang[5], Z. P. Zhang[43], Z. Y. Zhang[48], G. Zhao[1], J. W. Zhao[1], Lei Zhao[43], Ling Zhao[1], M. G. Zhao[28], Q. Zhao[1], Q. W. Zhao[1], S. J. Zhao[50], T. C. Zhao[1], Y. B. Zhao[1], Z. G. Zhao[43], A. Zhemchugov[22,f], B. Zheng[44], J. P. Zheng[1], Y. H. Zheng[39], B. Zhong[26], L. Zhou[1], Li Zhou[28], X. Zhou[48], X. K. Zhou[39], X. R. Zhou[43], X. Y. Zhou[1], K. Zhu[1], K. J. Zhu[1], X. L. Zhu[36], Y. C. Zhu[43], Y. S. Zhu[1], Z. A. Zhu[1], J. Zhuang[1], B. S. Zou[1], J. H. Zou[1]

(BESIII Collaboration)

[1] Institute of High Energy Physics, Beijing 100049, People's Republic of China
[2] Beihang University, Beijing 100191, People's Republic of China
[3] Bochum Ruhr-University, D-44780 Bochum, Germany
[4] Carnegie Mellon University, Pittsburgh, Pennsylvania 15213, USA
[5] Central China Normal University, Wuhan 430079, People's Republic of China

[6] China Center of Advanced Science and Technology, Beijing 100190, People's Republic of China

[7] COMSATS Institute of Information Technology, Lahore, Defence Road, Off Raiwind Road, 54000 Lahore, Pakistan

[8] G.I. Budker Institute of Nuclear Physics SB RAS (BINP), Novosibirsk 630090, Russia

[9] GSI Helmholtzcentre for Heavy Ion Research GmbH, D-64291 Darmstadt, Germany

[10] Guangxi Normal University, Guilin 541004, People's Republic of China

[11] GuangXi University, Nanning 530004, People's Republic of China

[12] Hangzhou Normal University, Hangzhou 310036, People's Republic of China

[13] Helmholtz Institute Mainz, Johann-Joachim-Becher-Weg 45, D-55099 Mainz, Germany

[14] Henan Normal University, Xinxiang 453007, People's Republic of China

[15] Henan University of Science and Technology, Luoyang 471003, People's Republic of China

[16] Huangshan College, Huangshan 245000, People's Republic of China

[17] Hunan University, Changsha 410082, People's Republic of China

[18] Indiana University, Bloomington, Indiana 47405, USA

[19] (A)INFN Laboratori Nazionali di Frascati, I-00044, Frascati, Italy; (B)INFN and University of Perugia, I-06100, Perugia, Italy

[20] (A)INFN Sezione di Ferrara, I-44122, Ferrara, Italy; (B)University of Ferrara, I-44122, Ferrara, Italy

[21] Johannes Gutenberg University of Mainz, Johann-Joachim-Becher-Weg 45, D-55099 Mainz, Germany

[22] Joint Institute for Nuclear Research, 141980 Dubna, Moscow region, Russia

[23] KVI, University of Groningen, NL-9747 AA Groningen, The Netherlands

[24] Lanzhou University, Lanzhou 730000, People's Republic of China

[25] Liaoning University, Shenyang 110036, People's Republic of China

[26] Nanjing Normal University, Nanjing 210023, People's Republic of China

[27] Nanjing University, Nanjing 210093, People's Republic of China

[28] Nankai University, Tianjin 300071, People's Republic of China

[29] Peking University, Beijing 100871, People's Republic of China

[30] Seoul National University, Seoul, 151-747 Korea

[31] Shandong University, Jinan 250100, People's Republic of China

[32] Shanxi University, Taiyuan 030006, People's Republic of China

[33] Sichuan University, Chengdu 610064, People's Republic of China

[34] Soochow University, Suzhou 215006, People's Republic of China

[35] Sun Yat-Sen University, Guangzhou 510275, People's Republic of China

[36] Tsinghua University, Beijing 100084, People's Republic of China

[37] (A)Ankara University, Dogol Caddesi, 06100 Tandogan, Ankara, Turkey; (B)Dogus University, 34722 Istanbul, Turkey; (C)Uludag University, 16059 Bursa, Turkey

[38] Universitaet Giessen, D-35392 Giessen, Germany

[39] University of Chinese Academy of Sciences, Beijing 100049, People's Republic of China

[40] University of Hawaii, Honolulu, Hawaii 96822, USA

[41] University of Minnesota, Minneapolis, Minnesota 55455, USA

[42] University of Rochester, Rochester, New York 14627, USA

[43] University of Science and Technology of China, Hefei 230026, People's Republic of China

[44] University of South China, Hengyang 421001, People's Republic of China

[45] University of the Punjab, Lahore-54590, Pakistan

[46] (A)University of Turin, I-10125, Turin, Italy; (B)University of Eastern Piedmont, I-15121, Alessandria, Italy; (C)INFN, I-10125, Turin, Italy

[47] Uppsala University, Box 516, SE-75120 Uppsala, Sweden

[48] Wuhan University, Wuhan 430072, People's Republic of China

[49] Zhejiang University, Hangzhou 310027, People's Republic of China

[50] Zhengzhou University, Zhengzhou 450001, People's Republic of China

[a] Also at the Novosibirsk State University, Novosibirsk, 630090, Russia

[b] Also at the Moscow Institute of Physics and Technology, Moscow 141700, Russia and at the Functional Electronics Laboratory, Tomsk State University, Tomsk, 634050, Russia

[c] Also at University of Texas at Dallas, Richardson, Texas 75083, USA

[d] Also at the PNPI, Gatchina 188300, Russia

^{e} Also at Bogazici University, 34342 Istanbul, Turkey

^{f} Also at the Moscow Institute of Physics and Technology, Moscow 141700, Russia

Using 2.25×10^8 J/ψ events collected with the BESIII detector at the BEPCII storage rings, we observe for the first time the process $J/\psi \to p\bar{p}a_0(980)$, $a_0(980) \to \pi^0\eta$ with a significance of 6.5σ (3.2σ including systematic uncertainties). The product branching fraction of $J/\psi \to p\bar{p}a_0(980) \to p\bar{p}\pi^0\eta$ is measured to be $(6.8 \pm 1.2 \pm 1.3) \times 10^{-5}$, where the first error is statistical and the second is systematic. This measurement provides information on the a_0 production near threshold coupling to $p\bar{p}$ and improves the understanding of the dynamics of J/ψ decays to four body processes.

I. INTRODUCTION

As one of the low-lying scalars, the state $a_0(980)$ has turned out to be mysterious in the quark model scenario. Its production near threshold allows tests of various hypotheses for its structure, including quark-antiquark [1], four quarks [2], $K\bar{K}$ molecule [3] and hybrid states [4]. The measurement of $J/\psi \to p\bar{p}a_0(980)$ is an additional observable constraining any phenomenological models trying to understand the nature of the $a_0(980)$.

A chiral unitary coupled channels approach of the Chiral perturbation theory (ChPT) [5–7] is applied in investigation of the four-body decays $J/\psi \to N\bar{N}MM$ process [8] where the N stands for a baryon and the M for a meson. In this approach, the process $J/\psi \to p\bar{p}\pi^0\eta$ is investigated with the $a_0(980)$ meson generated through final state interaction (FSI). The amplitude of this process is calculable except for some coefficients which are not restricted, and its branching fraction varies within a wide range for different coefficients. Therefore, an experimental measurement of the process $J/\psi \to p\bar{p}a_0(980) \to p\bar{p}\pi^0\eta$ is needed for further progress in understanding of the dynamics of the four-body decay processes taking the FSI of mesons into account.

In this paper, we present a measurement of $J/\psi \to p\bar{p}a_0(980)$ with $a_0(980)$ decaying to $\pi^0\eta$ based on 2.25×10^8 J/ψ events [9] collected with the BESIII detector at BEPCII.

II. THE EXPERIMENT AND DATA SETS

BESIII/BEPCII [10] is a major upgrade of BE-SII/BEPC [11]. BEPCII is a double-ring e^+e^- collider running at 2.0-4.6 GeV center-of-mass energies; it provides a peak luminosity of 0.4×10^{33} cm^{-2}s^{-1} at the center-of-mass energy of 3.097 GeV.

The cylindrical BESIII detector has an effective geometrical acceptance of 93% of 4π. It contains a small cell helium-based (40% He, 60% C_3H_8) main drift chamber (MDC) which has 43 cylindrical layers and provides an average single-hit resolution of 135 μm and momentum measurements of charged particles; a time-of-flight

system (TOF) consisting of 5 cm thick plastic scintillators, with 176 detectors of length 2.4 m in two layers in the barrel and 96 fan-shaped detectors in the end caps; an electromagnetic calorimeter (EMC) consisting of 6240 CsI(Tl) crystals in a cylindrical structure and two end caps, which is used to measure the energies of photons and electrons; and a muon system (MUC) consisting of Resistive Plate Chambers (RPC). The momentum resolution of the charged particle is 0.5% at 1 GeV/c in a 1 Tesla magnetic field. The energy loss (dE/dx) measurement provided by the MDC has a resolution of 6%. The time resolution of the TOF is 80 ps in the barrel detector and 110 ps in the end cap detectors. The energy resolution of EMC is 2.5% (5.0%) in the barrel (end caps).

Monte Carlo (MC) simulated events are used to determine the detection efficiency, optimize selection criteria, and estimate possible backgrounds. The GEANT4-based [12] simulation software BOOST [13] includes the geometric and material description of the BESIII detectors, the detector response and digitization models, as well as the tracking of the detector running conditions and performance. The J/ψ resonance is generated by KKMC [14] which is the event generator based on precise predictions of the Electroweak Standard Model for the process $e^+e^- \to f\bar{f} + n\gamma$, where $f = e$, μ, τ, u, d, c, s, b and n is an integer number ≥ 0. The subsequent decays are generated with EVTGEN [15] with branching fractions being set to the world average values according to the Particle Data Group (PDG) [16] and the remaining unmeasured decays are generated by LUNDCHARM [17]. A sample of 2.25×10^8 simulated events, corresponding to the luminosity of data, is used to study background processes from J/ψ decays ('inclusive backgrounds'). A signal MC sample with more than 10 times of the observed events in data for the process $J/\psi \to p\bar{p}a_0(980) \to p\bar{p}\pi^0\eta$ is generated, where the shape of the $a_0(980)$ is parameterized with the Flatté formula [18].

III. EVENT SELECTION

We select the process $J/\psi \to p\bar{p}\pi^0\eta$, with both π^0 and η decaying to two photons, for this analysis. A

good charged track is required to have good quality in the track fitting and be within the polar angle coverage of the MDC, i.e., $|\cos\theta| < 0.93$, and pass within 1 cm of the e^+e^- interaction point in the transverse direction to the beam line and within 10 cm of the interaction point along the beam axis. Since the charged track in this process has relatively low transverse momentum, charged particle identification (PID) is only based on the dE/dx information with the confidence level $\text{Prob}_{\text{PID}}(i)$ calculated for each particle hypothesis i ($i = \pi/K/p$). A charged track with $\text{Prob}_{\text{PID}}(p) > \text{Prob}_{\text{PID}}(K)$ and $\text{Prob}_{\text{PID}}(p) > \text{Prob}_{\text{PID}}(\pi)$ is identified as a proton or an antiproton candidate. Photon candidates are required to have a minimum energy deposition of 25 MeV in the barrel ($|\cos\theta| < 0.8$) of the EMC and 50 MeV in the end caps ($0.86 < |\cos\theta| < 0.92$) of the EMC. EMC timing requirements ($0 \leq T \leq 14$ in units of 50 ns) are used to suppress electronic noise and to remove showers unrelated to the event. At the event selection level, candidate events are required to have at least two good charged tracks with one proton and one antiproton being identified, and at least four good photons.

We then perform a kinematic fit which imposes energy and momentum conservation at the production vertex to combinations of one proton and one antiproton candidate and four photons. For events with more than four photons, we consider all possible four-photon combinations, and the one giving the smallest χ^2_{4C} for the kinematic fit is selected for further analysis. To improve the signal-to-background ratio, events with $\chi^2_{4C} < 35$ are accepted; this optimizes the figure of merit $S/\sqrt{S+B}$, where S and B are the numbers of MC simulated signal and inclusive background events respectively. The best photons pairing to π^0 and η in the four selected photons are selected by choosing the combination that gives the minimum χ^2-like variable

$$\chi^2_{\pi^0\eta} = \frac{(M_{\gamma_1\gamma_2} - M_{\pi^0})^2}{\sigma^2_{\pi^0}} + \frac{(M_{\gamma_3\gamma_4} - M_\eta)^2}{\sigma^2_\eta},$$

where $M_{\gamma\gamma}$ is the invariant mass of two photons after kinematic fit and $M_{\pi^0/\eta}$ is the π^0/η mass from PDG [16]. The mass resolutions for the π^0 and η, σ_{π^0} and σ_η are extracted by fitting the corresponding mass spectra in the signal MC sample; they are found to be 6.0 MeV/c^2 and 9.8 MeV/c^2 respectively. A MC study shows the rate of correct combination of photons is greater than 99% by using the $\chi^2_{\pi^0\eta}$ metric. To suppress $p\bar{p}\pi^0\pi^0$ final states surviving in the 4C fit, we select two-photon pairs giving a minimum $\chi^2_{\pi^0\pi^0} = \frac{(M_{\gamma_1\gamma_2} - M_{\pi^0})^2}{\sigma^2_{\pi^0}} + \frac{(M_{\gamma_3\gamma_4} - M_{\pi^0})^2}{\sigma^2_{\pi^0}}$ and reject events with $\chi^2_{\pi^0\pi^0}$ less than 100. Figure 1 shows the mass spectra of selected $\gamma\gamma$ pairs for data and MC, where $\gamma_1\gamma_2$ indicates π^0 candidates and $\gamma_3\gamma_4$ indicates η candidates. The hatched histograms represent MC shapes from backgrounds and signal, where the background shapes are normalized based on their branching fractions and the signal shape is normalized to the rest area of the histogram of the data. We then require the

mass of π^0 and η candidates to be within a 3σ window around their mean values.

IV. DATA ANALYSIS

The backgrounds contaminating the selected $J/\psi \to p\bar{p}\pi^0\eta$ candidates arise mainly from events with the same topology ($p\bar{p}\gamma\gamma\gamma\gamma$), events with an additional undetected photon ($p\bar{p}\gamma\gamma\gamma\gamma\gamma$), and events with a fake photon being reconstructed ($p\bar{p}\gamma\gamma\gamma$). The potential final states of background are categorized into four kinds: $p\bar{p}\pi^0\pi^0$, $p\bar{p}\pi^0\pi^0\gamma$, $p\bar{p}\pi^0\gamma$ and $p\bar{p}\pi^0\gamma\gamma$, where the $p\pi^0$ can be produced from intermediate states Σ or Δ, and $\gamma\pi^0$ can be produced from ω. Since the branching fractions for the exclusive background processes $J/\psi \to \Sigma^+\Sigma^-(\gamma)/\Delta^+\Delta^-(\gamma)/p\bar{p}\omega(n\gamma)$ have not yet been measured, we determine them from the same J/ψ data sample. The measurements are performed by requiring different numbers of photon candidates in one event and selecting the combination of $p\pi^0$ with invariant mass closest to the mass of Σ or Δ, or selecting the combination of $\gamma\pi^0$ closest to the mass of ω. The measured branching fractions are shown in Table I, where the uncertainty is statistical only. With the detection efficiency correction for the exclusive background satisfying the $p\bar{p}\pi^0\eta$ selection criteria, the contribution of the exclusive backgrounds is calculated to be 290 ± 19, which accounts for 4.3% of the surviving events found in data. The distributions of $M_{\pi^0\eta}$ for data and backgrounds after normalization are presented in Fig. 2. A structure around 1.0 GeV (Fig. 2(a)) in data is clearly visible, but is not seen significantly in the corresponding distribution of the exclusive backgrounds (Fig. 2(b)).

The studies of the mass spectra of $M_{p\pi^0}$ and $M_{p\eta}$ show that the processes with intermediate states of $N(1440)$, $N(1535)$ and $N(1650)$ are the dominant contributions to $J/\psi \to p\bar{p}\pi^0\eta$ where $N(1440)$ decays to $p\pi^0$, $N(1535)$ decays to $p\pi^0$ or $p\eta$, and $N(1650)$ decays to $p\eta$, with the charge-conjugate modes being implied. A simple partial wave analysis (PWA) by calculating the amplitudes of these processes according to their Feynman Diagrams [19] is applied to the surviving events in data. The maximum likelihood method is used to fit the branching fraction of these intermediate states and their interferences. Figure 3(a) shows the scatter plot of $M^2_{p\pi^0}$ versus $M^2_{\bar{p}\eta}$ in data, which is consistent with the scatter plot of $M^2_{p\pi^0}$ versus $M^2_{\bar{p}\eta}$ of the best fit result shown in Fig. 3(b). The interference between the processes with N^* and the $p\bar{p}a_0(980)$ is found to be very small and is neglected in the following. The yield of $J/\psi \to p\bar{p}a_0(980) \to p\bar{p}\pi^0\eta$ obtained by the PWA is within 1σ statistical deviation of that obtained by fitting the mass spectrum of $\pi^0\eta$ described below. When applying the PWA without the component $J/\psi \to p\bar{p}a_0(980)$, no enhancement around 1.0 GeV is observed in the MC projection of $\pi^0\eta$ mass spectrum, which indicates that the enhancement seen
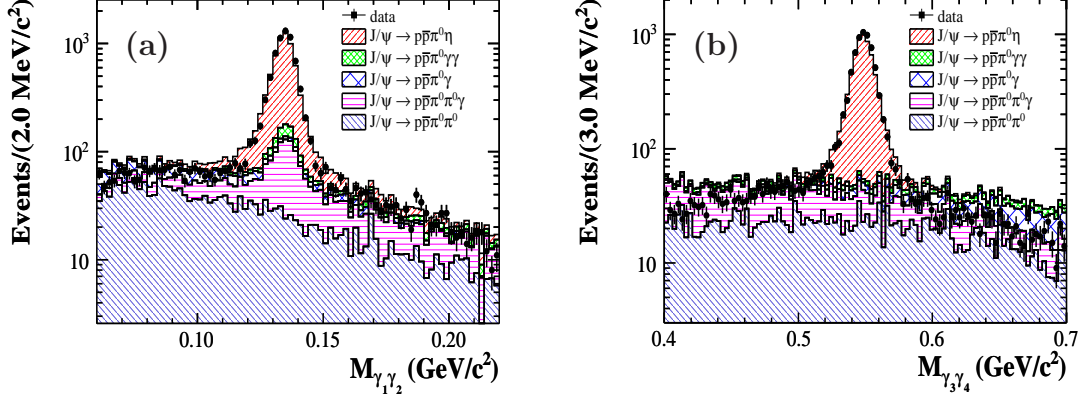
FIG. 1. The invariant mass distribution of (a) π^0 candidates and (b) η candidates. Dots with error bars are data. The hatched histograms are processes with different final states from simulated J/ψ decays.

TABLE I. Backgrounds of the final states with $p\bar{p}\pi^0\pi^0$, $p\bar{p}\pi^0\pi^0\gamma$, $p\bar{p}\pi^0\gamma$ and $p\bar{p}\pi^0\gamma\gamma$, where Br is the branching fraction of each channel, with statistical error only, ε_{MC}^{sel} is the selected efficiency of each channel determined with 50k MC sample, and N^{Norm} is the number of background events normalized to the total J/ψ data.

Channel($J/\psi \to$)	Br	ε_{MC}^{sel}	N^{Norm}
$p\bar{p}\pi^0\pi^0$	$(1.60 \pm 0.26) \times 10^{-3}$	1.68×10^{-4}	61 ± 10
$\Sigma^+\bar{\Sigma}^- \to p\pi^0\bar{p}\pi^0$	$(2.77 \pm 0.03) \times 10^{-4}$	1.26×10^{-4}	8 ± 0
$\Delta^+\bar{\Delta}^- \to p\pi^0\bar{p}\pi^0$	$(2.30 \pm 0.07) \times 10^{-4}$	1.76×10^{-4}	9 ± 0
$p\pi^0\bar{\Delta}^- + c.c \to p\pi^0\bar{p}\pi^0$	$(2.04 \pm 0.06) \times 10^{-4}$	1.76×10^{-4}	8 ± 0
$\gamma\Sigma^+\bar{\Sigma}^- \to \gamma p\pi^0\bar{p}\pi^0$	$(3.31 \pm 0.12) \times 10^{-5}$	2.98×10^{-3}	23 ± 1
$\gamma\Delta^+\bar{\Delta}^- \to \gamma p\pi^0\bar{p}\pi^0$	$(5.40 \pm 0.50) \times 10^{-5}$	2.86×10^{-3}	35 ± 3
$\gamma p\pi^0\bar{\Delta}^- + c.c \to \gamma p\pi^0\bar{p}\pi^0$	$(14.40 \pm 2.80) \times 10^{-5}$	2.44×10^{-3}	78 ± 15
$p\bar{p}\omega \to p\bar{p}\gamma\pi^0$	$(9.11 \pm 1.27) \times 10^{-5}$	1.59×10^{-3}	33 ± 5
$\gamma p\bar{p}\omega \to \gamma p\bar{p}\gamma\pi^0$	$(1.28 \pm 0.07) \times 10^{-5}$	1.14×10^{-2}	33 ± 2
$J/\psi \to p\bar{p}\eta', \eta' \to \gamma\omega, \omega \to \gamma\pi^0$	$(4.78 \pm 0.99) \times 10^{-7}$	1.80×10^{-2}	2 ± 0
Total			290 ± 19

in data is not from the processes with N^* intermediate states or their interferences.

An unbinned extended maximum likelihood fit is performed on the $\pi^0\eta$ mass spectrum. The probability density function (PDF) is

$$F(m) = f_{\text{sig}}\, \sigma(m) \otimes (\varepsilon(m) \times \hat{T}(m)) + (1 - f_{\text{sig}})\, B(m).$$

Here, f_{sig} is the fraction of $p\bar{p}a_0(980)$ signal events. The signal shape of $a_0(980)$ is described as an efficiency-weighted Flatté formula $(\varepsilon(m) \times \hat{T}(m))$ convoluted with a resolution function $\sigma(m)$. The non-$a_0(980)$ background shape, expressed by $B(m)$, is described by a third-order Chebychev polynomial function. The Flatté formula [18] is used to parameterize the $a_0(980)$ amplitudes coupling to $\pi^0\eta$ and $K\bar{K}$ by a two-channel resonance expressed as

$$\hat{T}(m) \propto \frac{1}{(m_{a_0}^2 - m^2)^2 + (\rho_{\pi^0\eta}g_{a_0\eta\pi^0}^2 + \rho_{K\bar{K}}g_{a_0K\bar{K}}^2)^2},$$

where $\rho_{\pi^0\eta}$ and $\rho_{K\bar{K}}$ are the decay momenta of the π^0 or

K in the $\pi^0\eta$ or $K\bar{K}$ rest frame, respectively. The two coupling constants $g_{a_0\pi^0\eta}$ and $g_{a_0K\bar{K}}$ stand for $a_0(980)$ resonance coupling to $\pi^0\eta$ and $K\bar{K}$, respectively. The experiment results from Refs. [20–22] are consistent with each other and the weighted average of them are calculated as $g_{a_0\pi^0\eta} = 2.83 \pm 0.05$ and $g_{a_0K\bar{K}} = 2.11 \pm 0.06$. In the fit, the two coupling constants $g_{a_0\pi^0\eta}$ and $g_{a_0K\bar{K}}$ are fixed to 2.83 and 2.11, respectively.

The mass-dependent efficiency $\varepsilon(m)$ is studied by using a large phase space MC $J/\psi \to p\bar{p}\pi^0\eta$ sample, where the efficiency curve derived from the four-body phase space MC is compatible with that from signal MC of $p\bar{p}a_0(980)$. The detector resolution $\sigma(m)$ of $M_{\pi^0\eta}$ is extracted by using a large sample of simulated signal events $J/\psi \to p\bar{p}a_0(980), a_0(980) \to \pi^0\eta$, with the width of the $a_0(980)$ set to zero.

In the fit, the signal fraction f_{sig}, the $a_0(980)$ mass, and the parameters of the background polynomial are allowed to vary. The fit result of $M_{\pi^0\eta}$ is shown in Fig. 4. The yield of $a_0(980)$ events is 849 ± 144, with
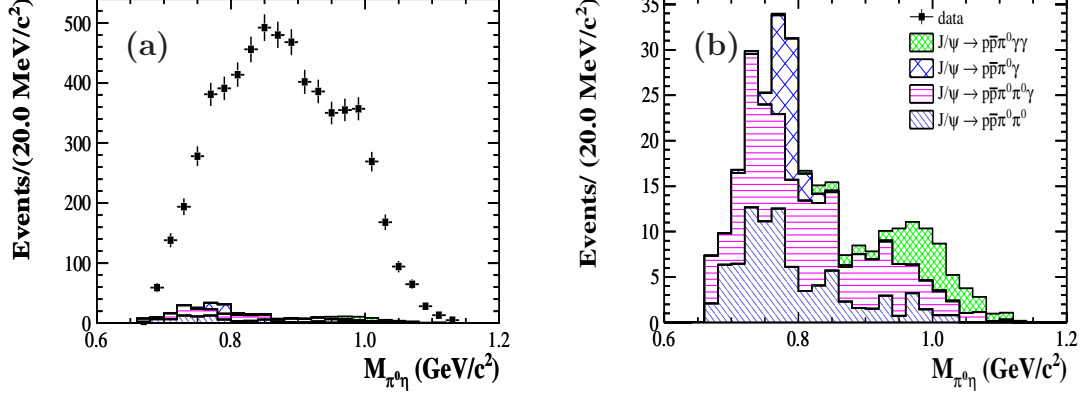
FIG. 2. (a) The mass spectrum of $\pi^0\eta$ for data and exclusive backgrounds. The dots with error bars represent data and the others are exclusive backgrounds after normalization. (b) The mass spectra of $\pi^0\eta$ for exclusive backgrounds.
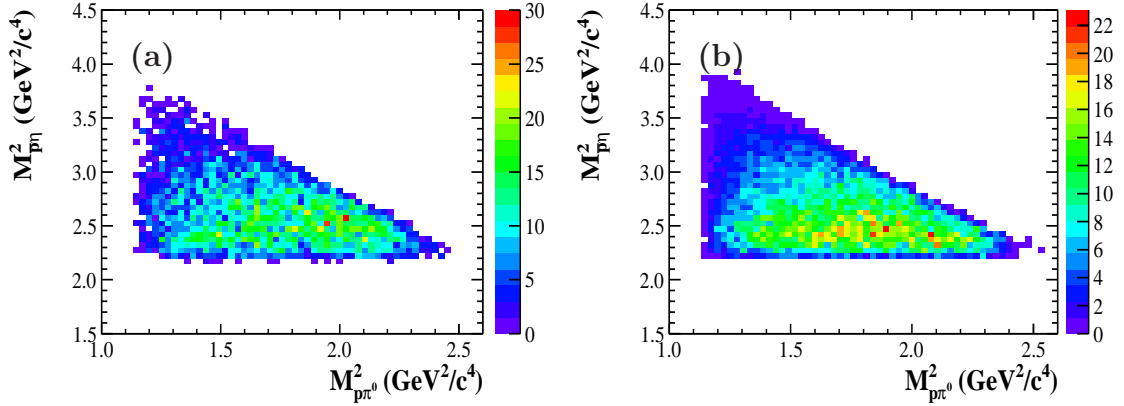

FIG. 3. (a) The scatter plot of $M^2_{p\pi^0}$ versus $M^2_{\bar{p}\eta}$ from data. (b) The scatter plot of $M^2_{p\pi^0}$ versus $M^2_{\bar{p}\eta}$ from MC projection of all intermediate states superimposed.

a statistical significance of 6.5σ which is calculated from the log-likelihood difference between fits with and without the $a_0(980)$ signal component. The fit mass is 1.012 ± 0.007 GeV/c^2, which is slightly higher than the PDG value [16]. The robustness of this result has been validated with a toy MC study. Different signal MC samples of $J/\psi \to p\bar{p}a_0(980)$, $a_0(980) \to \pi^0\eta$ are generated with different mass and width of the $a_0(980)$. Background events are randomly sampled according to the background shapes. In all cases, the fit value of the $a_0(980)$ mass is found to be consistent with the input value within statistical uncertainties. The product branching fraction $Br(J/\psi \to p\bar{p}a_0(980) \to p\bar{p}\pi^0\eta)$ is calculated to be $(6.8 \pm 1.2) \times 10^{-5}$, where the uncertainty is statistical only.

V. ESTIMATION OF SYSTEMATIC UNCERTAINTIES

The systematic uncertainties on the measurement of $Br(J/\psi \to p\bar{p}a_0(980) \to p\bar{p}\pi^0\eta)$ are summarized in Table II.

Systematic uncertainties due to tracking and PID efficiency, photon detection efficiency, the kinematic fit and the $\pi^0\pi^0$ veto arise due to imperfect modelling of the data by the simulation. The systematic uncertainty associated with the tracking efficiency as a function of transverse momentum and the uncertainty due to the PID efficiency of proton/antiproton have been studied by a control sample of $J/\psi \to p\bar{p}\pi^+\pi^-$ decays using a technique similar to that discussed in Ref. [23]. In this paper, due to the low transverse momentum of proton and antiproton, the uncertainty of tracking efficiency is determined by the weighted uncertainty $\Sigma_i \varepsilon_i r_i$, where ε_i
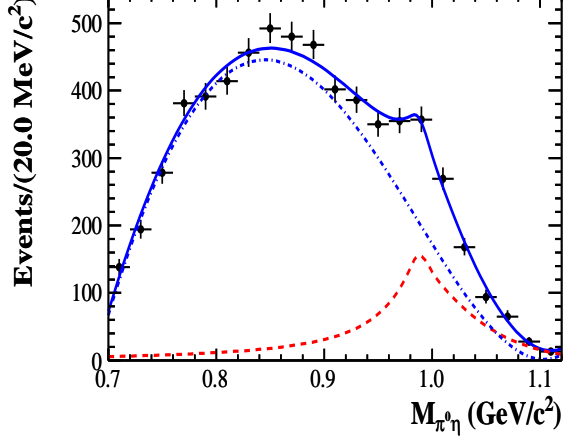
FIG. 4. The results of fitting the mass spectrum for $\pi^0\eta$. Dots with error bars are data and the solid line is the fitted spectrum. The dash-dotted line shows the non-$a_0(980)$ background described by a third-order Cheybechev polynomial. The dashed line shows the signal described by an efficiency-weighted Flatté formula convoluted with a resolution function.

TABLE II. Summary of systematic uncertainties on $Br(J/\psi \to p\bar{p}a_0(980) \to p\bar{p}\pi^0\eta)$.

Source	Uncertainty
Tracking	9.0%
Particle identification	4.0%
Photon detection	4.0%
4C kinematic fitting	3.2%
$\chi^2_{\pi^0\pi^0}$ cut	1.3%
Coupling constants	3.8%
Fit range	9.2%
Background shape	12.6%
Number of J/ψ events	1.2%
Total	19.6%

represents the data/MC difference in each transverse momentum bin [23] and r_i represents the proportion of each transverse momentum bin in data. The systematic uncertainty due to the tracking efficiency is estimated to be 4.0% per proton and 5.0% per antiproton, respectively. The large uncertainty of tracking efficiency is because of limited statistics in control sample and improper simulation of interactions with material for low momentum proton and antiproton. The uncertainty due to PID efficiency is 2.0% per proton or antiproton.

The systematic uncertainty due to photon detection is 1.0% per photon. This is determined from studies of the photon detection efficiency in the control sample $J/\psi \to \rho^0\pi^0$ [23].

To estimate the uncertainty from the kinematic fit, the efficiency of the selection on the χ^2_{4C} of the kinematic fit is studied using events of the decay $J/\psi \to p\bar{p}\eta$, $\eta \to \pi^0\pi^0\pi^0$. The uncertainty associated with the kinematic fit is determined by the difference of efficiencies for MC and data, and is estimated to be 3.2% for $\chi^2_{4C} < 35$.

The systematic uncertainty arising from the $\pi^0\pi^0$ veto metric ($\chi^2_{\pi^0\pi^0} > 100$) is studied by a control sample $J/\psi \to \omega\eta \to \pi^+\pi^-\pi^0\eta$. The control sample is selected due to its similar final states to signal, high statistics, and narrow ω/η signals to extract the efficiency precisely. To better model the signal process $J/\psi \to p\bar{p}a_0(980) \to p\bar{p}\pi^0\eta$, the $\chi^2_{\pi^0\pi^0}$ distribution of control sample is weighted to that of signal process. The event number of control sample is extracted by fitting invariant mass of $\pi^+\pi^-\pi^0$ with a double Gaussian function, and the efficiency for $\chi^2_{\pi^0\pi^0}$ requirement is ratio of the number of events that with and without veto metric, to be $(97.4 \pm 1.0)\%$ and $(97.6 \pm 0.4)\%$ for data and MC, respectively, where the errors are statistical only. Conservatively, the systematic uncertainty of $\chi^2_{\pi^0\pi^0}$ veto metric is estimated to be 1.3%.

The systematic uncertainty due to the signal shape is determined by varying the coupling constants by 1σ within their center values for $g_{a_0\pi^0\eta}$ and $g_{a_0 K\bar{K}}$ separately. The largest difference is taken as the uncertainty.

To study the uncertainty from background, alternative background shapes are obtained by varying the fitting range from [0.7, 1.12] GeV/c² to [0.73, 1.12] GeV/c² and changing order of Chebychev polynomial from third-order to fourth-order, which introduce uncertainties of 9.2% and 12.6%, respectively.

The systematic uncertainty of the total number of J/ψ events is obtained by studying inclusive hadronic J/ψ decays [9] to be 1.2%.

We treat all the sources of systematic uncertainties as uncorrelated and sum them in quadrature to obtain the total systematic uncertainty.

VI. CONCLUSION AND DISCUSSION

Based on 2.25×10^8 J/ψ events collected with the BESIII detector at BEPCII, we observe $J/\psi \to p\bar{p}a_0(980)$, $a_0(980) \to \pi^0\eta$ for the first time with a statistical significance of 6.5σ. Taking the systematic uncertainty into account, the significance is 3.2σ. Without considering the interference between the signal channel and the same final states with intermediate N^* states, the branching fraction is measured to be

$$Br(J/\psi \to p\bar{p}a_0(980) \to p\bar{p}\pi^0\eta) = (6.8 \pm 1.2 \pm 1.3) \times 10^{-5},$$

where the first uncertainty is statistical and the second is systematic.

Our measurement provides a quantitative comparison with the chiral unitary approach [8]. This approxima-

tion uses several coefficients in the parametrization of meson-meson amplitudes. One of them, namely r_4 in [8], is constrained by fitting the $\pi^+\pi^-$ invariant mass distribution in the decay $J/\psi \to p\bar{p}\pi^+\pi^-$; the fit suggests two equally possible values, $r_4 = 0.2$ and $r_4 = -0.27$. The theory also predicts that the branching fractions of $J/\psi \to p\bar{p}a_0(980)$ and $J/\psi \to p\bar{p}\pi^+\pi^-$ are comparable for $r_4 = -0.27$, while the branching fraction of the former is one or two orders of magnitude lower than that of the latter for $r_4 = 0.2$. Taking the branching fraction of $J/\psi \to p\bar{p}\pi^+\pi^-$ from PDG [16], the ratio of $Br(J/\psi \to p\bar{p}a_0(980) \to p\bar{p}\pi^0\eta)$ to $Br(J/\psi \to p\bar{p}\pi^+\pi^-)$ is found to be about 10^{-2}, which shows preference to $r_4 = 0.2$.

[1] N. N. Achasov and V. N. Ivanchenko, Nucl. Phys. B **315**, 465 (1989).

[2] J. Weinstein, N. Isgur, Phys. Rev. D **27**, 588 (1983).

[3] J. Weinstein, N. Isgur, Phys. Rev. D **41**, 2236 (1990).

[4] S. Ishida *et al.*, the 6th International conference on Hadron Spectroscopy, 1995.

[5] S. Weinberg, Physica A **96**, 327 (1979).

[6] V. Bernard, N. Kaiser and U.-G. Meissner, Int. J. Mod. Phys. E **4**, 193 (1995).

[7] A. Pich, Rep. Prog. Phys. **58**, 563 (1995).

[8] C. B. Li, E. Oset, and M. J. Vicente Vacas, Phys. ReV. C **69**, 015201 (2004).

[9] M. Ablikim *et al.* (BESIII Collaboration), Chin. Phys. C **36**, 915 (2012).

[10] M. Ablikim *et al.* (BESIII Collaboration), Nucl. Instr. Meth. A **614**, 345 (2010).

[11] J. Z. Bai *et al.* (BES Collaboration), Nucl. Instr. Meth. A **458**, 637 (2001).

[12] S. Agostinelli *et al.* (Geant4 Collaboration), Nucl. Instr. Meth. A **506**, 250 (2003).

[13] Z. Y. Deng *et al.*, HEP & NP **30**, 371 (2006).

[14] S. Jadach, B. F. L. Ward and Z. Was, Comput. Phys. Commun. **130**, 260 (2000); Phys. Rev. D **63**, 113009 (2001).

[15] R. G. Ping, Chin. Phys. C **32**, 599 (2008); D. J. Lange, Nucl. Instr. Meth. A **462**, 152 (2001).

[16] J. Beringer *et al.* (Particle Data Group), Phys. Rev. D **86**, 010001 (2012).

[17] J. C. Chen *et al.*, Phys. Rev. D **62**, 034003 (2000).

[18] S. M. Flatté, Phys. Lett. B **63**, 224 (1976).

[19] J. X. Wang, Nucl. Instr. Meth. A **534**, 241 (2004).

[20] S. Teige *et al.* (E852 Collaboration), Phys. Rev. D **59**, 012001 (1998).

[21] F. Ambrosina *et al.*, Phys. Lett. B **681**, 5 (2009).

[22] D. V. Bugg, Phys. Rev. D **78**, 074023 (2008).

[23] M. Ablikim *et al.* (BESIII Collaboration), Phys. Rev. D **83**, 112005 (2011).